Al-Mustansiriyah Journal of Science
ISSN: 1814-635X (print), ISSN:2521-3520 (online) Volume 31, Issue 2, 2020 DOI: http://doi.org/10.23851/mjs.v31i2.694

Research Article **Open Access**

New stabilizer Cellulose Nano Rods-Zinc Oxide (CNR-ZnO) material for nanocomposite synthesis and anti-bacterial applications

Wisam J. Aziz, Randa K. Hussain, Ibrahim Abbas Ibrahim*

Department of Physics, College of Science, Mustansiriyah University, Baghdad, IRAQ.

*Correspondent author email: ibraheem.abbas87@uomustansiriyah.edu.iq

ArticleInfo

Received
08/07/2019

Accepted
25/11/2019

Published
15/04/2020

ABSTRACT

Zinc oxide (ZnO) nanorods were fabricated using Cellulose Nano Rods (CNR) as a new stabilizer material. Synthesized of ZnO-CNR nanocomposites, with a molar ratio of ZnO to CNR (1/2g) were prepared in distilled water. The nanocomposites were distinguished using X-ray diffraction (XRD), ultraviolet-visible (UV-Vis), and Field Emission scanning electron microscope (FESEM) techniques. XRD data were showed, the ZnO nanorods with a hexagonal wurtzite structure such readily scattered inside CNR with an average size 20-40nm. (FESEM) images showed the homogenous morphology of Zinc oxide rods. The optimum ratio of ZnO-CNR was selected to be the tiny size of the ZnO nanorods that yielded a good stabilizer material and antibacterial activity. The ultraviolet-visible (UV-Vis) absorption spectrum of the ZnO-CNR nanocomposites appeared absorption peaks in the ultraviolet region at (350-360 nm) wavelength attributes with the energy gap of (3.41eV) of ZnO-CNR. The antibacterial activities of samples have been investigated against the Gram-positive (pneumonia) and gram-negative (pseudomonas). The maximum antibacterial activities against the Gram-positive (pneumonia) of ZnO nanorods and of ZnO- cellulose nanorods are 16mm and 22mm respectively. The optimum anti-bacterial activities versus the Gram-negative (pseudomonas) of zinc oxide nanorods and zinc oxide- cellulose nanorods are 17mm and 19mm respectively. The optimum anti-bacterial activities versus the Gram-negative (pseudomonas) of zinc oxide nanosheet and of zinc oxide-cellulose nanorods are 17mm and 22mm.

KEYWORDS: ZnO; Nanocomposite; Cellulose nano rods; stabilizer material; antibacterial activity.

الخلاصة

أوكسيد الزنك النانوي (ZnO) تم خلطه مع قضبان السليلوز النانوية (CNR) واستخدم السيليلوز كمادة مثبته جديدة. تم تصنيع مركبات أوكسيد الزنك – السيليلوزالنانوية بنسب مولية لاوكسيد الزنك (ZnO) (ZnO-CNR) والسيليلوز (CNR) (٢/١ غرام) تم تحضيرها في الماء المقطر. تم دراسة الخصائص البصرية للمركبات النانوية باستخدام الأشعة فوق البنفسجية المرئية (UV-Vis) و الخصائص التركيبية باستخدام حيود الأشعة السينية (XRD) و المجهر الإلكتروني المساح (FESEM). تم عرض بيانات (XRD)، وقضبان أوكسيد الزنك النانوي (ZnO) ذات تركيب (wurtzite) سداسي وكان الحجم الحبيبي للبلوزة هو بين ٢٠-٤٠ نانومتر. وأظهرت الصور (FESEM) اشكال متجانسة لقضبان أوكسيد الزنك. تم اختيار النسبة المثلى من (ZnO-CNR) بناءً على الحجم الصغير لقضبان أوكسيد الزنك النانوي (ZnO) التي أسفرت عن مادة ثبات جيدة وذات نشاط مضاد للجراثيم جيد. أظهرت أطياف امتصاص الأشعة فوق البنفسجية لمركبات (ZnO-CNR) النانوية قمم الامتصاص في منطقة الأشعة فوق البنفسجية (٣٥٠-٣٦٠ نانومتر) التي تعزى إلى فجوة النطاق (3.41 eV) لاوكسيد الزنك – سيليلوز (ZnO-CNR) . تم التحقق في الأنشطة المضادة للجراثيم من العينات ضد بكتريا موجبة الجرام (*pneumonia*) وسالبة الجرام (*pseudomonas*). الحد الأقصى للأنشطة المضادة للبكتيريا ضد بكتريا موجبة الجرام (*pneumonia*) الرئوي) لقضبان أوكسيد الزنك النانوي (ZnO) وقضبان أوكسيد الزنك - السليلوز هي ١٦ ملم و ٢٢ ملم على التوالي. الحد الأقصى للأنشطة المضادة للبكتيريا ضد بكتريا سالبة الجرام (*pseudomonas*) لقضبان أوكسيد الزنك النانوي (ZnO) وقضبان أوكسيد الزنك -سيليلوز هي ١٧ ملم و ١٩ ملم على التوالي.

INTRODUCTION

Zinc oxide is a semi-conductor material that is very significant in many applications, like solar cells, transparent windows, gas sensors, photo catalysts, laser diodes and acoustic wave devices[1]. Zinc oxide has a wide energy gap of (3.3 eV), weak resistivity and height transparency in the visible range. ZnO nano rods have been mainly synthesis by many methods such as: sputtering[2], chemical vapor deposition[3], sol-

gel process[4], drop-casting and spray pyrolysis[5]. Drop casting; is a good technique because it is characterized by a simplicity, effectively and not contaminating production[6].
Nano-sized cellulose has a good properties such as large aspect ratio[7], good dissolvability in water[8], mechanical properties[9], minimal thermal degradation behavior[10], and a high ability for the absorption of metallic particles[11]. It is used in bioenergy, chemical reaction, catalytic, and biomedical applications[12]. In most studies, Cellulose Nano Crystal (CNC) has been applied as a reinforcing phase to improve the chemical and physical properties of materials. Recently, cellulose CNC has been used as a substrate to fabricate nano-sized metallic particles[13]. Cellulose nanocrystals (CNCs) are crystalline nano-rods with a thickness of 3–10 nm and a length of a few hundred nanometers[14]. They are extracted from pulp fibers using an acid-mediated procedure, which has already been industrialized[15]. (CNCs) can also be extracted directly from wood and lignocelluloses using a variety of reagents and processes[16]. CNCs of a length in the micrometers can also be obtained from tunicate cellulose[17]. In the present study, ZnO nanoparticles were prepared with Cellulose Nano Rod (CNR) in order to stop the formation of aggregated ZnO nano particles and improve the stability and antibacterial activity of nano particle dispersion. The ZnO-cellulose nanocomposite was obtained in the form of a white crystalline powder[18]. The use of antibacterial agents is necessary to prevent microorganism growth and reduce the harmful effects in our life at the same time[19, 20]. Inorganic antimicrobial agents are promising such as metal salts, nano-sized metals and metal oxides[21, 22].

EXPERIMENTAL METHODS

Materials

The purity and origin of the product are shown in Table 1.

Preparation of Cellulose Nano-rods

The cellulose powder harvested from (2 g) hydrolyzed with a sulfuric acid solution (20 mL, 64 w/w%) at 45 °C for 60 min. The resultant suspension was diluted 10-fold with cold water (6 °C) followed by centrifuging and dialysis until getting a neutral pH = (7). Finally, the sample located inside the fridge to make freeze-dried.

Table 1. Properties of materials were used.

Material	Origin	Specifications (purity) %
Cellulose powder	Germany	(99.99)
Sulfuric acid	Germany/ Scharlau	(98)
Ethanol	USA/Sigma Aldrich	(100)
Sodium hydroxide	Newzealand/ AjaxFinechem	(97)
(Zn $(NO_3)_2$.$6H_2O$)	Germany	(99.99)

Preparation zinc oxide nano rods

The zinc oxide (ZnO) nano rods were prepared from 1 g of zinc nitrate ($Zn(NO_3)_2.6H_2O$ 99.9%) was dissolved in 10 ml of distilled water. The zinc nitrate solution will be formed. The sodium hydroxide solution was prepared from1 1 g of sodium hydroxide dissolved in 5 ml distilled water. Zinc nitrate with sodium was mixed then the mixture has been located on hot plate stirr at 60 °C for 6 h to fully blend the mixture. The mixture was placed in the centrifuge with repeated washing two times to remove the sodium hydroxide residues. The liquid mixture was deposited on a glass slide using drop-casting method. The slide is placed on a hot plate at 500 °C for 3 h to obtain the zinc oxide nano particle[23].

Preparation ZnO-CNR

The precipitation of zinc oxide precipitate and the cellulose was mixed with each other by magnetic stirring. The weight ratios of ZnO: CNR nanocomposites were (1:2) g put in the centrifuge and washing by distilled water to remove the extra CNR. After complete washing, the specimen was dried at 100 °C for 6 h to complete the conversion of the remaining zinc hydroxide to zinc oxide[23].

RESULTS AND DISCUSSION

X-ray diffraction

Figure 1 reveals ZnO film of ten pronounced diffraction peaks, (31.7, 34.4, 36.2, 47.5, 56.6, 62.8, 67.9,68.2, 69.0 and 77.8 of 2 theta scale) corresponding to (100), (002), (101), (102), (110) (103), (202), (112), (201) (004) and (202) planes of the crystallized wurtzite structure of ZnO respectively. Figure 2 shows the XRD of cellulose film with three pronounced diffraction peaks at 2θ = (16.3◦, 22.6◦, and 34.7◦) corresponds to the (1 0 1), (0 0 2), and (004) crystallographic planes, respectively. Figure 3 show XRD cellulose which represent the pronounced diffraction peaks of

16.3, 22.6, 34.4, corresponds to the (1 0 1), (0 0 2), and (0 4 0) crystallographic planes and ZnO diffraction peaks which represent the pronounced diffraction peaks (31.7, 34.4, 36.2, 47.5, 56.6, 62.8, 67.9,68.2, 69.0 and 77.8 of 2 theta scale) corresponding to (100), (002), (101), (102) , (110) (103), (202), (112), (201), (004) and (202) planes. The narrow full width at half-maximum (FWHM) of the peaks corresponding to the samples of ZnO, cellulose and ZnO- CNR, these are good to crystalize form. Crystalline sizes are calculated using the Scherrer equation (1)[24]. Support this explanation the XRD results which reveal the broadening of FWHM peaks lead to a decrease in crystal size. This happened because the inversely effect of full width half maximum on the crystal size as shown in Table 2 [25, 26].

$$D = 0 \cdot 9\lambda/(\beta cos\theta) \quad (1)$$

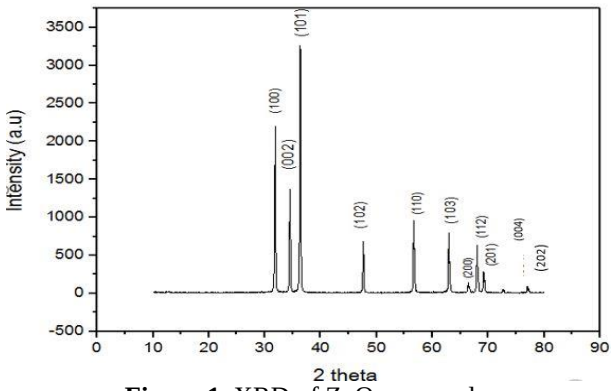

Figure 1. XRD of ZnO nano rods.

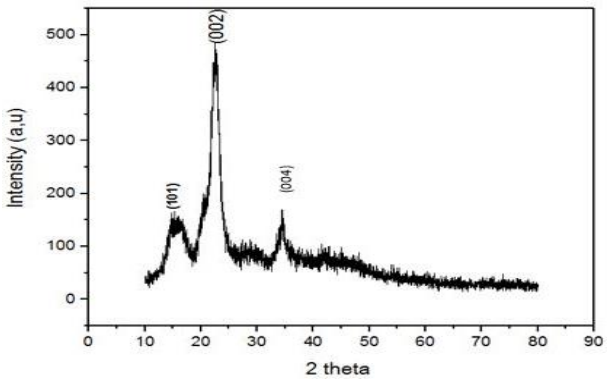

Figure 2. XRD of pure cellulose powder.

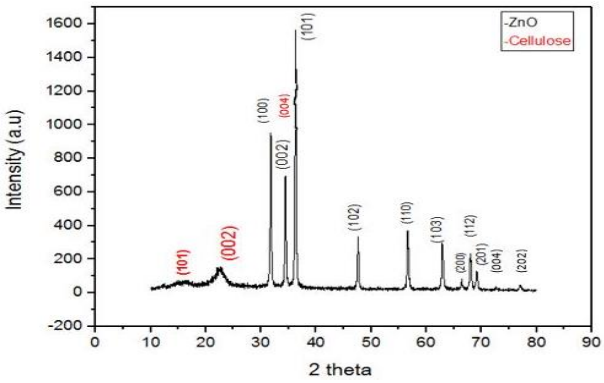

Figure 3. XRD of ZnO-cellulose nano rods.

Table 2. The Crystal size, full width at half maximum, and diffraction angle of cellulose and ZnO films deposited on glass substrates.

Material	Crystal size (nm)	2theta (deg)	FWHM (deg)
Cellulose	1.67	22.58	4.82
ZnO	0.2224	36.30	37.40

Morphological properties

Figure 4 shows the FESEM images of pure ZnO nano rods, cellulose, and ZnO–cellulose nano rods deposited on glass substrates. Field Emission Scanning Electron Microscopy (FESEM) is a convenient technique to show a close-packed morphology for both ZnO and ZnO-cellulose nano rods, which decrease in grain size. The treatment of cellulose powder with both ZnO and NaOH solutions led to the nucleation and growth of discrete ZnO seeds at the cellulose surfaces.

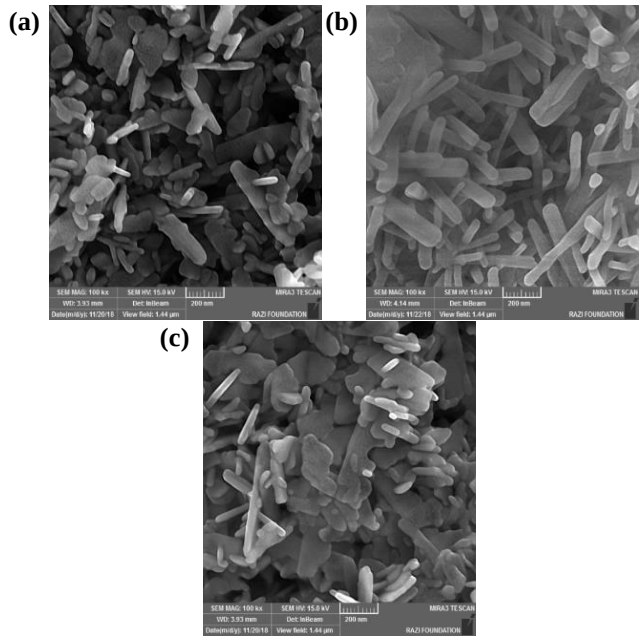

Figure 4. FESEM images of (a) pure ZnO nano rods (b) pure cellulose and (c) ZnO – cellulose nano rods.

Optical properties

UV-Vis absorption spectrum

UV-vis absorption spectrum of ZnO nano rods is shown in Figure 5. The excitation absorption peaks of the samples were in a range of 275 to 320 nm. The UV-Vis absorption spectrum of ZnO-cellulose nano rods is shown in Figure 6. The absorption peaks of the samples are in a range of 350 to 360 nm. The increased surface area of nano rods and their uniform distribution on the cellulose surface might increase the UV absorption efficiency.

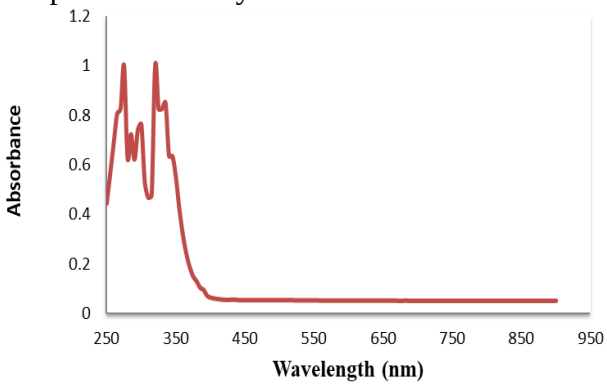

Figure 5. UV-Vis absorption spectrum of ZnO nano rods.

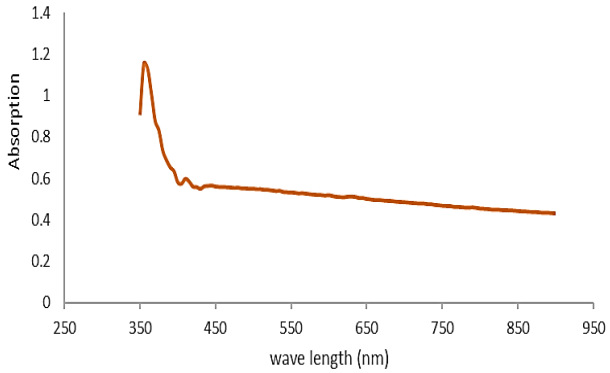

Figure 6. UV-Vis absorbance spectrum of ZnO – cellulose nano rods.

Energy band gap

The direct band gap of ZnO nano rods estimated from a plot of $(\alpha h\upsilon)^2$ versus the photon energy ($h\upsilon$) is 3.16 eV as shown in Figure 7.

Figure 8 shows the direct band gap of ZnO with CNR nanocomposite which equal 3.4 eV. There is a small increase in the energy band gap, due to the addition of cellulose. Polymers have a wide energy band gap, and that is the bigger band gap bulk which is increase nano formatting, as a result conclude to increasing band gap of the ZnO.

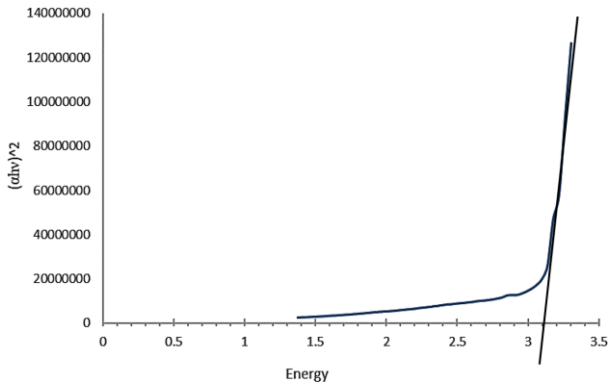

Figure 7. Energy band gap of ZnO nano rods.

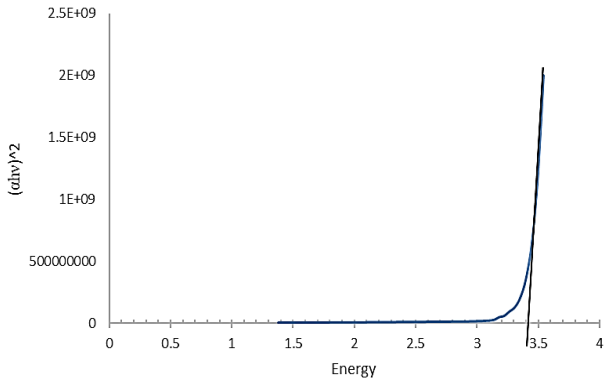

Figure 8. Energy band gap of ZnO nano– cellulose nano rods.

Antibacterial activity

The antibacterial activities were carried out by the disc diffusion method. Antimicrobial activities of samples (ZnO nano rods, and ZnO-Cellulose nano rods) have been investigated against the Gram-positive (*pneumonia*) and gram-negative (*pseudomonas*). The maximum antibacterial activities against the Gram-positive (*pneumonia*) of ZnO nano rods and of ZnO- cellulose nano rods are 17 mm and 22 mm respectively. The maximum antibacterial activities against the Gram-negative (*pseudomonas*) of ZnO nano rods and ZnO- cellulose nano rods are 17 mm and 19 mm respectively. The antibiotic Gentamicin **(**CN) was applied to Gram-positive (*pneumonia*) and found that the killing area of antibiotic

(Gentamicin CN) is 17 mm either for *pseudomonas*, the antibiotic (genemycin) did not kill the bacteria but was discouraged and the area of discouraged was (20 D) mm where (D) is inhibition zone and the antibiotic (Erythromycin (E)) did not give any effect on gram-negative and gram-positive bacteria indicated an enhancement by composition of ZnO- cellulose nano rods. The area of killing for all types of positive, negative bacteria and antibiotic (Gentamicin),

(Erythromycin (E)) is shown in Table 2, Figure 9 and Figure 10.

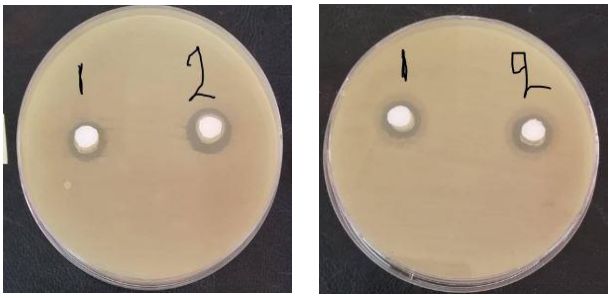

(a) *Pneumonia* (b) *Pseudomonas*

Figure 1. Optical micrographs of agar plates, showing the variation in the zone of inhibition zone a (1), b (1) ZnO nano rods a (2), b (2) ZnO-cellulose nano rod.

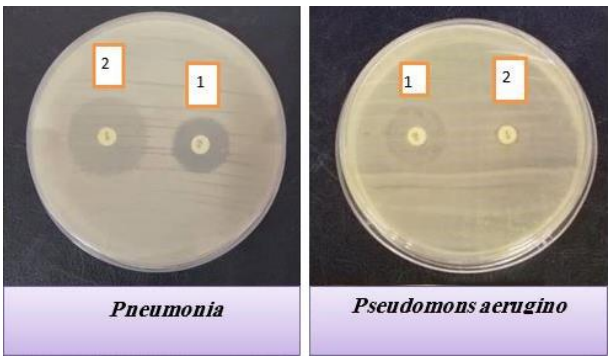

Figure 10. Optical micrographs of agar plates, showing the inhibition zone of 1- Gentamicin 2- Erythromycin.

Table 2. show antibacterial activity of ZnO, ZnO-cellulose nano rods.

N	compounds	*Pneumonia*	*Pseudomons aerugino*
1	ZnO	17	17
2	ZnO-cellulose	22	19
3	Cellulose	-	-
4	Antibiotic Gentamicin (CN)	17	20 D
5	Antibiotic Erythromycin (E)	-	-

CONCLUSION

ZnO nano rods with a hexagonal wurtzite structure and average crystal size around 30 nm were successfully prepared with CNR using a drop-casting method. Optimum zinc oxide peak was at 2 theta 36.6 corresponding to (101) while for the cellulose was 22.8 corresponds to (002) and the two peaks (101) (002) were optimum as the highest peaks of Zinc Oxide – Cellulose. In SEM images the surfaces of ZnO nano rods were relatively homogenous. These nano rods are interlaced with each other, which create an excellent absorbance. The UV-Vis for ZnO-cellulose nano rods synthesized at 100 °C was observed at 360 nm which is higher than of pure ZnO. The cellulose was crucial for the improvement of the porosity of the ZnO surface responsible for enhanced absorption of UV radiation. The energy band gaps were 3.16 eV and 3.41 eV of ZnO and ZnO-CNR nano rods respectively.

The homogenous dispersion of ZnO in polymer blend matrix CNR, it can be concluded that the stabilization of ZnO nano rods by cellulose nano rods could help to increase their dispersion in the polymer blend matrix and prevents agglomerations.

REFERENCES

[1] J. Löffler, R. Groenen, J. L. Linden, M. C. M. van de Sanden, and R. E. I. Schropp, "Amorphous silicon solar cells on natively textured ZnO grown by PECVD," *Thin Solid Films*, vol. 392, no. 2, pp. 315-319, 2001/07/30/ 2001.

[2] M. Purica, E. Budianu, E. Rusu, M. Danila, and R. Gavrila, "Optical and structural investigation of ZnO thin films prepared by chemical vapor deposition (CVD)," *Thin Solid Films*, vol. 403-404, pp. 485-488, 2002/02/01/ 2002.

[3] D. Bao, H. Gu, and A. Kuang, "Sol-gel-derived c-axis oriented ZnO thin films," *Thin Solid Films*, vol. 312, no. 1, pp. 37-39, 1998/01/14/ 1998.

[4] Z. M. Jarzebski, "Preparation and physical properties of transparent conducting oxide films," *physica status solidi (a)*, vol. 71, no. 1, pp. 13-41, 1982/05/16 1982.

[5] S. Studenikin, N. Golego, and M. J. J. o. A. P. Cocivera, "Optical and electrical properties of undoped ZnO films grown by spray pyrolysis of zinc nitrate solution," vol. 83, no. 4, pp. 2104-2111, 1998.

[6] R. Ayouchi, D. Leinen, Martı, x, F. n, M. Gabas, E. Dalchiele, and J. R. Ramos-Barrado, "Preparation and characterization of transparent ZnO thin films obtained by spray pyrolysis," *Thin Solid Films*, vol. 426, no. 1, pp. 68-77, 2003/02/24/ 2003.

[7] M. M. De Souza Lima, J. T. Wong, M. Paillet, R. Borsali, and R. Pecora, "Translational and Rotational Dynamics of Rodlike Cellulose Whiskers," *Langmuir*, vol. 19, no. 1, pp. 24-29, 2003/01/01 2003.

[8] Y. Shin, I.-T. Bae, B. W. Arey, and G. J. Exarhos, "Facile Stabilization of Gold-silver Alloy Nanoparticles on Cellulose Nanocrystal," *The Journal of Physical Chemistry C*, vol. 112, no. 13, pp. 4844-4848, 2008/04/01 2008.

[9] A. Šturcová, G. R. Davies, and S. J. Eichhorn, "Elastic Modulus and Stress-Transfer Properties of Tunicate Cellulose Whiskers," *Biomacromolecules*, vol. 6, no. 2, pp. 1055-1061, 2005/03/01 2005.

[10] T. Nishino, I. Matsuda, and K. Hirao, "All-Cellulose Composite," *Macromolecules*, vol. 37, no. 20, pp. 7683-7687, 2004/10/01 2004.

[11] J. He, T. Kunitake, and A. Nakao, "Facile In Situ Synthesis of Noble Metal Nanoparticles in Porous Cellulose Fibers," *Chemistry of Materials*, vol. 15, no. 23, pp. 4401-4406, 2003/11/01 2003.

[12] H. Liu, D. Wang, Z. Song, and S. Shang, "Preparation of silver nanoparticles on cellulose nanocrystals and the application in electrochemical detection of DNA hybridization," *Cellulose*, vol. 18, no. 1, pp. 67-74, 2011/02/01 2011.

[13] J. Cai, S. Kimura, M. Wada, and S. Kuga, "Nanoporous Cellulose as Metal Nanoparticles Support," *Biomacromolecules*, vol. 10, no. 1, pp. 87-94, 2009/01/12 2009.

[14] "Standard Terms and Their Definition for Cellulose Nanomaterial," 2017.

[15] D. Bondeson, A. Mathew, and K. J. C. Oksman, "Optimization of the isolation of nanocrystals from microcrystalline cellulose by acid hydrolysis," vol. 13, no. 2, p. 171, 2006.

[16] H. Abushammala, R. Goldsztayn, A. Leao, and M.-P. Laborie, "Combining steam explosion with 1-ethyl-3-methylimidazlium acetate treatment of wood yields lignin-coated cellulose nanocrystals of high aspect ratio," *Cellulose*, vol. 23, no. 3, pp. 1813-1823, 2016/06/01 2016.

[17] I. A. Sacui, R. C. Nieuwendaal, D. J. Burnett, S. J. Stranick, M. Jorfi, C. Weder, E. J. Foster, R. T. Olsson, and J. W. Gilman, "Comparison of the Properties of Cellulose Nanocrystals and Cellulose Nanofibrils Isolated from Bacteria, Tunicate, and Wood Processed Using Acid, Enzymatic, Mechanical, and Oxidative Methods," *ACS Applied Materials & Interfaces*, vol. 6, no. 9, pp. 6127-6138, 2014/05/14 2014.

[18] K. Sahoo and J. Nayak, "ZnO-cellulose nanocomposite powder for application in UV sensors," in *AIP Conference Proceedings*, 2017, vol. 1832, no. 1, p. 050090: AIP Publishing.

[19] F. Paladini, M. Pollini, A. Sannino, and L. Ambrosio, "Metal-Based Antibacterial Substrates for Biomedical Applications," *Biomacromolecules*, vol. 16, no. 7, pp. 1873-1885, 2015/07/13 2015.

[20] Z. Sharifalhoseini, M. H. Entezari, and R. Jalal, "Evaluation of antibacterial activity of anticorrosive electroless Ni–P coating against Escherichia coli and its enhancement by deposition of sono-synthesized ZnO nanoparticles," *Surface and Coatings Technology*, vol. 266, pp. 160-166, 2015/03/25/ 2015.

[21] N. A. Ibrahim, T. M. Abou Elmaaty, B. M. Eid, and E. Abd El-Aziz, "Combined antimicrobial finishing and pigment printing of cotton/polyester blends," *Carbohydrate Polymers*, vol. 95, no. 1, pp. 379-388, 2013/06/05/ 2013.

[22] P. Petkova, A. Francesko, M. M. Fernandes, E. Mendoza, I. Perelshtein, A. Gedanken, and T. Tzanov, "Sonochemical Coating of Textiles with Hybrid ZnO/Chitosan Antimicrobial Nanoparticles," *ACS Applied Materials & Interfaces*, vol. 6, no. 2, pp. 1164-1172, 2014/01/22 2014.

[23] H. R. Ghorbani, F. P. Mehr, H. Pazoki, and B. M. J. O. J. o. C. Rahmani, "Synthesis of ZnO nanoparticles by precipitation method," vol. 31, no. 2, pp. 1219-1221, 2015.

[24] S. Abbas, K. Hussain, Z. Hussain, R. Ali, and T. J. P. A. A. Abbas, "Anti-Bacterial Activity of Different Soaps Available in Local Market of Rawalpindi (Pakistan) against Daily Encountered Bacteria," vol. 7, no. 522, p. 2, 2016.

[25] O. Tobail, "Porous silicon for thin solar cell fabrication," 2008.

[26] J. Ma, F. Ji, H.-l. Ma, and S.-y. Li, "Preparation and properties of transparent conducting zinc oxide and aluminium-doped zinc oxide films prepared by evaporating method," *Solar Energy Materials and Solar Cells*, vol. 60, no. 4, pp. 341-348, 2000/02/01/ 2000.